Comparative Biochemistry and Physiology, Part B 165 (2013) 165–171

Contents lists available at SciVerse ScienceDirect

Comparative Biochemistry and Physiology, Part B

journal homepage: www.elsevier.com/locate/cbpb

Characterization of cDNAs for calmodulin and calmodulin-like protein in the freshwater mussel *Hyriopsis cumingii*: Differential expression in response to environmental Ca^{2+} and calcium binding of recombinant proteins

Gang Ren [a,b], Xiaolong Hu [a], Jinyu Tang [a], Yan Wang [a,*]

[a] College of Animal Sciences, Zhejiang University, Hangzhou 310058, China
[b] College of Life Science, Shaoxing University, Shaoxing 312000, China

ARTICLE INFO

Article history:
Received 5 February 2013
Received in revised form 12 April 2013
Accepted 13 April 2013
Available online 18 April 2013

Keywords:
Hyriopsis cumingii
*Hc*CaM and *Hc*CaLP
Gene expression
Calcium metabolism
Calcium stimulation

ABSTRACT

Calmodulin and calmodulin-like protein are two crucial calcium regulators in bivalves. However, molecular characteristics and expression patterns of these genes in the freshwater mussel are poorly understood. In this study, two cDNAs encoding novel calmodulin and calmodulin-like protein (*Hc*CaM and *Hc*CaLP) were cloned and characterized from the freshwater pearl mussel *Hyriopsis cumingii*. The full-length cDNA of *Hc*CaM was 726 bp, including a 118-bp 5′-untranslated region (UTR), a 447-bp open reading frame (ORF), and a 161-bp 3′-UTR. The 1217-bp *Hc*CaLP cDNA comprised of a 51-bp 5′-UTR, a 447-bp ORF, and a 716-bp 3′-UTR. The potential phosphorylation sites of, Arg^{80} and Phe^{100} in deduced HcCaM were mutated to Thr^{80} and Tyr^{100} in HcCaLP. Tissue-specific expression analysis revealed that *Hc*CaM mRNA was prominently expressed in the gill, mantle center, and foot. In contrast, *Hc*CaLP mRNA was mainly expressed in the mantle edge. The recombinant HcCaM and HcCaLP proteins expressed in *Escherichia coli* showed the typical Ca^{2+} dependent electrophoretic shift characterization as CaM and differed in the calcium binding affinity. The calcium stimulation test that lasted 5 weeks implied that *Hc*CaM and *Hc*CaLP had differential expression patterns in response to various environmental Ca^{2+} concentrations (0.25–1.25 mM). The expression of *Hc*CaM mRNA was up-regulated by low Ca^{2+} concentration (0.25 mM), and the highest expression of HcCaLP mRNA occurred under Ca^{2+} concentration of 1 mM.

1. Introduction

Bivalve shell consists of calcium carbonate, matrix proteins and other organic matrices, and calcium carbonate accounts for approximately 95% of shell weight. Biomineralization of bivalve shell is regulated by calcium metabolism, including the sequential processes of calcium absorption, accumulation, transportation, and incorporation (Huang et al., 2007; Machado and Lopes-Lima, 2011). Calcium metabolism is controlled by many Ca^{2+} regulators, such as calcitonin (Breimer et al., 1988), troponin C (Ojima et al., 1994), calmodulin (CaM) (Li et al., 2004), calmodulin-like protein (CaLP) (Li et al., 2005), and calconectin (Duplat et al., 2006). CaM is a crucial and ubiquitous calcium sensor protein in eukaryotes and mediates cellular functions by interacting with numerous target proteins, including calcineurin, myosin light chain kinases, and phosphorylase kinase in various metabolic and signaling pathways (Friedberg and Rhoads, 2001; Ikura and Ames, 2006). In marine bivalves, CaM is a regulator of the membrane Ca^{2+}-ATPase system that is responsible for uptake, transportation, and secretion of Ca^{2+} in the gill and mantle (Stommel et al., 1982; Stommel and Stephens, 1985; Li et al., 2004). Calmodulin-like protein (CaLP), another member of the CaM superfamily, has been identified in a wide range of organisms from bacteria to mammals (Nikapitiya et al., 2010). CaLP acts as a multifunctional calcium sensor and regulates calcium metabolism in various processes, such as Ca^{2+} transportation in buffalo sperm (Sidhu and Guraya, 1993), epithelial cell differentiation in humans (Rogers et al., 2001), and shell formation in pearl oyster *Pinctada fucata* (Li et al., 2005). As a component of the organic layer in bivalve shell, CaLP also induces the nucleation of aragonite through binding with the 16-kDa nacre protein, and regulates the growth of calcite in the prismatic layer or participates in the shell regeneration (Yan et al., 2007; Fang et al., 2008). To date, the presence of multiple *CaM* and *CaLP* genes has been observed in marine molluscs (Li et al., 2004; Li et al., 2005; Simpson et al., 2005).

Calcium metabolism pattern is obviously different between freshwater and marine bivalves due to the Ca^{2+} concentration difference in freshwater and seawater (Richardson et al., 1981). Earlier studies reported that increasing calcium availability can enhance calcium

* Corresponding author at: Department of Applied Zoology, College of Animal Sciences, Zhejiang University, Hangzhou 310058, China. Tel./fax: +86 571 88982891.
E-mail address: ywang@zju.edu.cn (Y. Wang).

1096-4959/$ – see front matter © 2013 Elsevier Inc. All rights reserved.
http://dx.doi.org/10.1016/j.cbpb.2013.04.003

deposition in shell of freshwater mussels (Wilbur and Jodrey, 1952; Dalesman and Lukowiak, 2010). However, few calcium regulators have been reported from freshwater bivalves, and the molecular mechanism of calcium metabolism in freshwater mussels is not clear (Zeng et al., 2012). In the present study, we isolated and characterized full length cDNAs of two calcium regulators, *Hc*CaM and *Hc*CaLP from freshwater pearl mussel *Hyriopsis cumingii*, which contributes more than 95% pearl yield in the world (Wang et al., 2009). We also tested the differential expression of *Hc*CaM and *Hc*CaLP under different environmental Ca^{2+} concentrations.

2. Materials and methods

2.1. Mussel and sample collection

Mussels from a commercial freshwater pearl mussel farm at Fengqiao, Zhuji (Zhejiang, China) were collected during the fast growth stage in September, 2012. Six mussels including 3 1-year-old mussels and 3 2-year-old mussels were sampled, and 9 samples were isolated from each mussel for tissue expression profiling, including gill (GL), intestine (IN), foot (FT), gonad (GN), adductor muscle (AM), mantle center (MC), mantle edge (ME), posterior of mantle pallial (pMP), and middle of mantle pallial (mMp). The samples were frozen in liquid nitrogen and stored at −80 °C.

2.2. Rapid amplification of cDNA ends (RACE)

Total RNA was extracted from the mantle pallial of 2-year-old mussels using TRIzol Reagent (Invitrogen, Carlsbad, CA, USA) according to the manufacturer protocol, and then quantified by measuring absorbance at 260 nm with a NanoDrop 2000 spectrophotometer (Thermo Scientific, Wilmington, DE, USA). The full-length cDNAs of *Hc*CaM and *Hc*CaLP were synthesized from total RNA using the SMART™ RACE cDNA Amplification Kit (Clontech, PaloAlto, CA, USA) according to the manufacturer's instructions. To obtain the 3′ terminal sequence of the *Hc*CaM and *Hc*CaLP cDNA ends, the forward primer HcCaMF1 was designed based on the conserved regions in the open reading fragment (ORF) of *H. schlegelii Hs*CaM cDNA sequence (GenBank Accession No. FJ194962) and a *H. cumingii* EST sequence (GW692024) (Table 1). 3′-RACE PCR was performed in a 50-μL reaction mixture comprising 1.0 μL of Advantage 2 Polymerase Mix (Clontech, PaloAlto, CA, USA), 5.0 μL of Advantage 2 PCR Buffer, 1.0 μL of *Hc*CaMF2 primer (10 μM), 5 μL of universal primer mix (UPM, 10×), and 2.5 μg of total RNA. PCR products were electrophoresed on a 1.2% agarose gel and stained with ErBr. Bands of approximately 700 bp and 1200 bp were excised from the gel respectively, purified using a DNA Fragment Purification Kit (TaKaRa, Dalian, China), and subsequently cloned into a pMD19-T vector using a TA cloning kit (TaKaRa) and sequenced. Based on the 3′-cDNA end sequences of *Hc*CaM and *Hc*CaLP, gene-specific primers were designed for two rounds of 5′-RACE PCR and listed in Table 1. PCR of 5′-cDNA ends and cloning of the products were carried out as described above for 3′-cDNA ends.

Table 1
Primers and their applications in this study.

Primer name	Sequence 5′ → 3′	Use
HcCaMF1	GGAGGCGTTCAGCCTGTTT	3′ RACE
HcCaMR1	AACAACATTTGCATTACTTATGCCCTTCCAC	1st round 5′ RACE
HcCaMR2	TGCCCTTCCACAGCTCTATCTCCTTATTGT	2nd round 5′ RACE
HcCaLPR1	AACTTCGGTGAAGCGGAAAAGGATTTG	1st round 5′ RACE
HcCaLPR2	GGAATTCKGGGAAATCWATCGTKCCATT	2nd round 5′ RACE
HcCaLPF3	TTTCACTTCCATAACACCTGCT	ORF amplification
HcCaLPR3	AACTTCGGTGAAGCGGAAAAGGATTTG	ORF amplification
RT-HcCaMF	GCAGCAGAACTCAGACACGTGAT	Realtime PCR forward
RT-HcCaMR	CCCTTCCACAGCTCTATCTCCTTAT	Realtime PCR reverse
RT-HcCaLPF	CAAATCCTTTTCCGCTTCACC	Realtime PCR forward
RT-HcCaLPR	CGTTGTTGACATTGCTCCAGAA	Realtime PCR reverse
RC-HcCaMF	ATGGCTGACCAACTGACGGAAGAAC	Domain amplification
RC-HcCaMR	TTATTTACTCGTCATCATCTGCACG	Amplification domain and positive recombinant clone
RC-HcCaLPF	ATGGCAGACCAACTAACAGAAGAAC	Domain amplification
RC-HcCaLPR	TCACTTCGACATCATCATCCTCACG	Amplification of domain and positive recombinant clone
actin-F	CCCTGGAATCGCTGACCGTAT	Realtime PCR forward
actin-R	GCTGGAAGGTGGAGAGAGAAG	Realtime PCR reverse
T7 Promoter	TAATACGACTCACTATA	Recombinant clone amplification

2.3. Sequence analysis

Determination of the gene, ORF, and protein sequence was performed using the Expert Protein Analysis System (ExPASy, http://au.expasy.org). Multiple sequence alignments were analyzed using the Cluster W 1.81 (Thompson et al., 1994). Domain prediction was undertaken using the simple modular architecture research tool (SMART, http://smart.embl-heidelberg.de/). The prediction of phosphorylation sites was carried out by NetPhos 2.0 Server (http://www.cbs.dtu.dk/services/NetPhos/).

2.4. Tissue specific expression of the HcCaM and HcCaLP genes

Expression analysis was performed by real-time quantitative PCR using the iQTM5 Multicolor Real-Time PCR Detection System Cycler (BioRad, Hercules, CA, USA). Total RNA was extracted with TRIzol Reagent (Invitrogen). cDNA from total RNA was synthesized by a PrimeScript® Reverse Transcriptase kit (TaKaRa), using oligo $(dT)_{18}$ as primer. Gene-specific primers, RT-HcCaMF and RT-HcCaMR for PCR were designed based on the 3′ terminal region of ORF and 3′-UTR sequence of *Hc*CaM mRNA respectively, and RT-CaLPF and RT-HcCaLPR on the 3′-UTR sequences of *Hc*CaLP mRNA (Table 1). *β-actin* was used as endogenous reference gene for calibration, and primers actin-F and actin-R were designed according to the *β-actin* cDNA sequence (GenBank Accession No. HM045420) (Table 1).

Real-time quantitative PCR was performed with the SYBR® Premix Ex Taq™ PCR kit (TaKaRa). Amplifications were performed in 25 μL. An aliquot of 1.0 μL of the cDNA synthesized above was used as template. The cycling conditions for *Hc*CaM, *Hc*CaLP and *β-actin* were the same as follows: 1 min at 95 °C, followed by 40 cycles (95 °C for 30 s, 56 °C for 30 s, and 72 °C for 30 s). Melting curves were also performed with 0.5 °C increments from 50 °C to 95 °C to ensure that a single PCR product was amplified using each pair of primers. The relative mRNA levels were normalized to *β-actin* transcripts using the following formula $N = 2^{(Ct\ \beta\text{-actin} - Ct\ \text{target gene})}$.

2.5. Recombination and protein purification of HcCaM and HcCaLP

The full coding regions of *Hc*CaM and *Hc*CaLP were amplified using the primers of RC-HcCaMF/R and RC-HcCaLPF/R separately (Table 1), and were ligated to the expression vector pEASY-E1 (TransGen Biotech, Beijing, China). The recombinant plasmids, pEASY-E1-HcCaM and pEASY-E1-HcCaLP were transformed into Trans1-T1 phage resistant chemically competent cell of *Escherichia coli* (TransGen Biotech). The forward positive clones were screened by PCR with vector primer T7 promoter primer and recombinant reverse primers (Table 1), and further confirmed by sequencing. The positive recombinant plasmid, pEASY-E1-HcCaM and pEASY-E1-HcCaLP, were isolated by AxyPrep ™ Plasmid Miniprep Kit (Axygen Biosciences, Union City, Ca, USA) and transferred into *E. coli* BL21 (DE3) (TransGen Biotech), incubated in LB medium. The *E. coli* BL21 (DE3) inserted pEASYE1 vector without insert fragment was also cultured in LB medium as negative control. Protein expression was induced for 4 h after addition of 1.0 mM isopropyl β-D-1-thiogalactopyranoside (IPTG) at 37 °C. The

purification and identification of recombinant proteins, HcCaM and HcCaLP, followed the method described in Li et al. (2005).

2.6. Ca^{2+}-dependent electrophoretic mobility shift assay

Ca^{2+} dependent electrophoretic shift assay was performed using the method described in Burgess et al. (1980). Purified recombinant proteins HcCaM and HcCaLP (5 μg) were mixed with the sample buffer containing 0.2 mM $CaCl_2$ or EGTA. Samples were electrophoresed simultaneously in two SDS gels containing 5 mM $CaCl_2$ and 5 mM EGTA respectively, and thereafter stained by Coomassie Brilliant Blue R-250.

2.7. Calcium stimulation experiment

The calcium stimulation experiment was conducted in five 500-liter polyethylene tanks. In each tank, six 1-year-old *H. cumingii* (shell length 82 ± 2 mm, mean ± SD, n = 6) were co-cultured with five grass carp *Ctenopharyngodon idellus* (body mass 200 ± 10 g) and five Prussian carp *Carassius (auratus) gibelio* (body mass 150 ± 10 g). Five Ca^{2+} concentrations, 0.25, 0.5, 0.75, 1, and 1.25 mM, were established by adding $CaCl_2$ into the tanks. During the experiment, the fish were fed a commercial formulated fish feed (Kesheng Feed Co., Ltd., Shaoxing, China) once daily, and Ca^{2+} concentration was monitored twice weekly with the method described by Wei (2002). To evaluate nacre deposition, a plastic sheet (5 × 3 mm) was inserted into the mantle cavity between shell and mantle pallial in each side of the mussel. The experiment lasted for 5 weeks, during which water temperature fluctuated within 20 to 24 °C. Mass gain of the mussels was calculated as final mussel mass − initial mussel mass. Nacre deposited on the plastic sheet was incised from shell along the edges of plastic sheet, detached from plastic sheet, and thereby was weighed on an electronic balance. Nacre deposition was calculated as nacre deposited on the plastic sheet (1 mm^2)/duration of the experiment. At the end of the experiment, gill and mantle edge were sampled from each mussel and the samples (n = 6) were frozen in liquid nitrogen and stored at −80 °C. The expression profiles of *Hc*CaM and *Hc*CaLP mRNA were detected with the qRT-PCR method mentioned above.

2.8. Statistical analysis

The amount of *Hc*CaM and *Hc*CaLP mRNA was normalized to that of *β-actin* mRNA in the same sample. The differences of mRNA expression levels in tissues and age were examined with two-way ANOVA with Tukey's HSD test. The differences in mRNA expression levels, mass gain, and nacre deposition among the Ca^{2+} concentrations (in the Calcium stimulation experiment section) were examined with one-way ANOVA, and further comparison was performed with Tukey's HSD test. The statistical analysis was performed using the SPSS software (version 19.0). Significance level was set at $P < 0.05$.

3. Results

3.1. Full-length cDNAs of HcCaM and HcCaLP

The *Hc*CaM cDNA had a full-length of 726 bp, which included a 118-bp 5′-UTR, a 447-bp ORF, and a 161-bp 3′-UTR. The 1217-bp *Hc*CaLP cDNA comprised of a 51-bp 5′-UTR, a 447-bp ORF, and a 716-bp 3′-UTR (Fig. 1). Putative polyadenylation signals (AATAAA) were recognized at the nucleotide positions at 672 bp of *Hc*CaM cDNA and 1171 bp of *Hc*CaLP cDNA. Sequence similarity between the *Hc*CaM and *Hc*CaLP ORF nucleotide sequences was 79.6%. Both full-length cDNA sequences were deposited in GenBank (*Hc*CaM, GenBank Accession No. JQ389856; *Hc*CaLP, JQ389857).

3.2. Predicted protein sequences of HcCaM and HcCaLP

The deduced HcCaM and HcCaLP proteins both contained 149 amino acids. Multiple sequence alignment of HcCaM and HcCaLP revealed that these two proteins had a high homology, with 87.2% identity. In addition, both proteins contained four putative Ca^{2+}-binding EF-hand motifs, with positions at 12–40 aa, 48–76 aa, 85–113 aa, and 121–149 aa (Fig. 2). According to the tertiary structures built by SWISS-MODEL, both proteins comprised two globular domains and a central 11-residue loop-linker that tethered the globular domains. Comparing the variance in amino acid sequences revealed that the mutated amino acid residues were highly concentrated in the central loop-linker, such as 80 aa and 82 aa which were homologous to two crucial phosphorylation sites, Thr^{79} and Ser^{81}, in human CaM (PDB ID: 1CLL). Arg^{80} and Ser^{82} in *H. cumingii* HcCaM are substituted by Thr^{80} and Thr^{82} in HcCaLP respectively. In addition, another important mutation site between HcCaM and HcCaLP is the 100th aa, which is Phe^{100} in HcCaM substituted by Tyr^{100} in HcCaLP.

3.3. Tissue expression of HcCaM and HcCaLP mRNA

The tissue-specific expression of *Hc*CaM and *Hc*CaLP in the pMP, mMP, MC, ME, GN, IN, AM, GL, and FT of *H. cumingii* of 1 year old or 2 years old was determined by real-time PCR using β-actin as an internal control. The tissue-specific expression pattern of *Hc*CaM and *Hc*CaLP had no significant difference in 1- and 2-year-old mussels. *Hc*CaM mRNA was detected in all the tissues, and expressed at high levels in the MC, ME, GL, and FT, whereas expression level of *Hc*CaLP mRNA was high in the ME, detectable in the pMP, mMP, MC, and GL, and low in the FT and AM (Fig. 3).

3.4. Ca^{2+}-dependent electrophoretic shift analysis

HcCaM and HcCaLP were over expressed as an N-terminal His-tag fusion protein using *E. coli*, and purified using immobilized nickel metal ion affinity chromatography. To confirm the purified proteins as CaM and CaLP and to investigate the difference of their calcium binding affinity, the electrophoretic mobility shift of proteins upon Ca^{2+} binding was tested. The electrophoretic mobility of HcCaM and HcCaLP was higher in the presence of Ca^{2+} and lower in the presence of EGTA, whereas the extent of shift differed between HcCaM and HcCaLP (Fig. 4). The difference between molecular masses of recombinant HcCaM identified by the Ca^{2+} gel and that identified by EGTA gel was approximately 1.5 kDa, whereas the value was approximately 3.3 kDa for recombinant HcCaLP.

3.5. Expression of HcCaM and HcCaLP mRNA under different Ca^{2+} concentrations

Nacre deposition in the mussels was highest at the Ca^{2+} concentration of 0.75 mM, but no significant difference was found in mass gain between the mussels reared under different Ca^{2+} concentrations (Fig. 5). The expression level of *Hc*CaM mRNA in the GL was highest at the Ca^{2+} concentration of 0.25 mM ($P < 0.01$), and it was also higher at the Ca^{2+} concentration of 0.75 mM than at the Ca^{2+} concentration of 0.5, 1, and 1.25 mM (Fig. 6, $P < 0.05$). The expression level of *Hc*CaLP mRNA in the ME was highest at the Ca^{2+} concentration of 1 mM ($P < 0.05$).

4. Discussion

In the present study, we cloned a novel *CaM* gene, *Hc*CaM and a novel *CaLP* gene, *Hc*CaLP from freshwater mussel *H. cumingii*. It is the first report that multiple *CaM* and *CaLP* genes exist in freshwater mussel. Compared with the deduced protein sequences, an important phosphorylation site Tyr^{100} in the Ca^{2+}-binding ligand position Z of

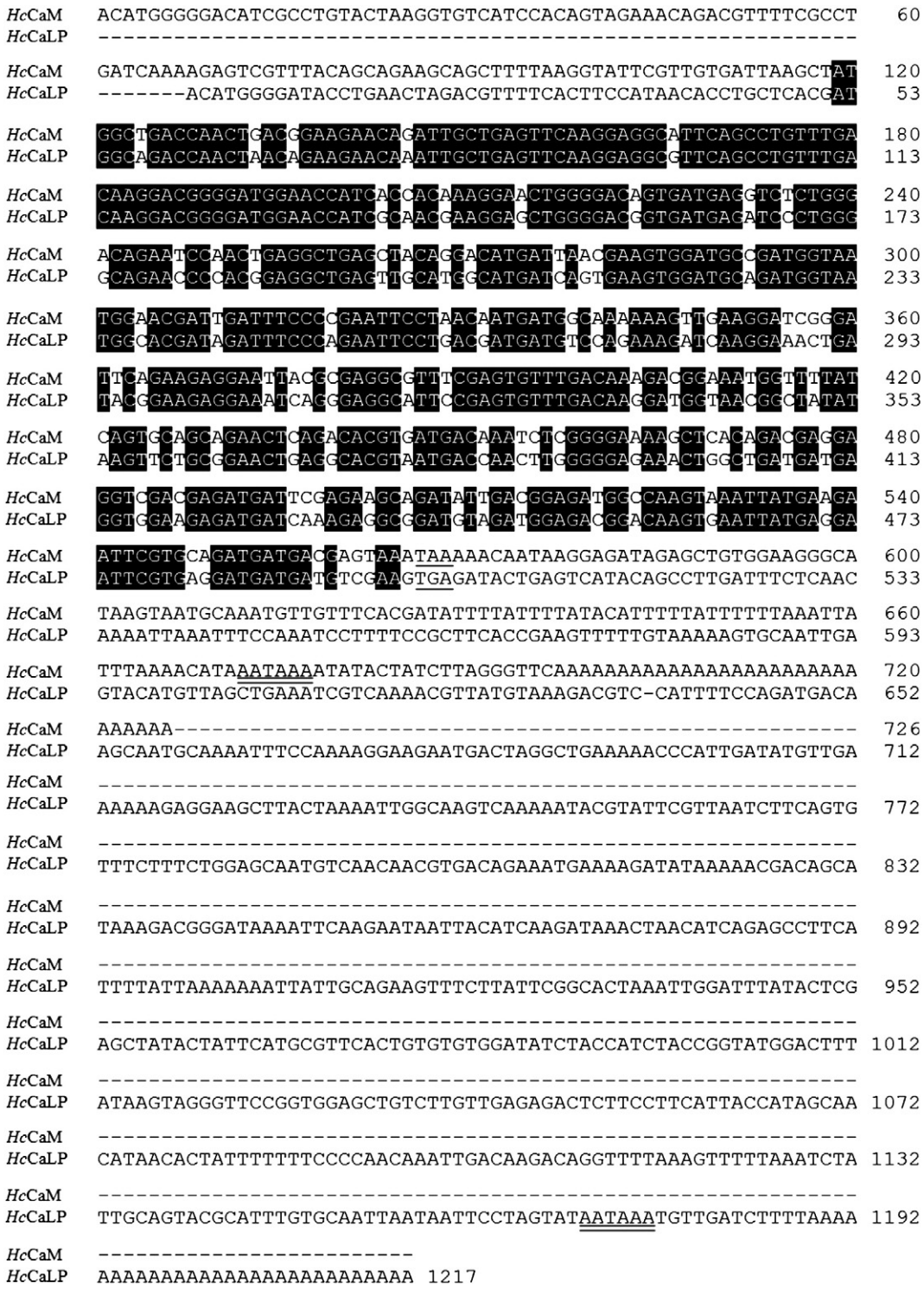

Fig. 1. Nucleotide sequences of full-length *Hc*CaM and *Hc*CaLP cDNAs. The identical nucleotide sites in open reading frames (ORFs) of cDNAs are shaded. The stop codons and consensus polyadenylated signal sites are underlined with single lines and double lines, respectively.

the third EF-hand motif of HcCaLP was substituted by Phe^{100} in HcCaM. Like human CaMs, phosphorylation of Tyr^{100} in HcCaLP might increase binding affinity for its target proteins (Corti et al., 1999). The substitution in phosphorylation sites of 100 aa might provide differential regulation of HcCaM and HcCaLP at the post-transcriptional level (Toutenhoofd and Strehler, 2000). Differential Ca^{2+} affinity is one of the main factors reducing the different functions in CaMs and CaLPs (Lee et al., 2000; Hoeflich and Ikura, 2002). Ca^{2+}-dependent electrophoretic shift analysis suggested that the recombinant HcCaLP had higher Ca^{2+} affinity than recombinant HcCaM. The increase in affinity of HcCaLP for Ca^{2+} would induce a conformational change of this protein, and enhance its affinity for most of its target proteins and its ability to activate target proteins (Kilhoffer et al., 1983; Hoeflich and Ikura, 2002).

CaM is of importance in regulation of Ca^{2+} absorption in bivalves (Stommel et al., 1982; Stommel and Stephens, 1985; Li et al., 2004). In the present study, the expression level of *Hc*CaM mRNA was similar in the gill, mantle center, and foot of *H. cumingii*, suggesting that the

```
                    20                  40                  60
H.cumingii CaM  MADQLTEEQIAEFKEAFSLFDKDGDGTITTKELGTVMRSLGQNPTEAELQDMINEVDADGNGTIDFPEFLTMMAKK 76
H.cumingii CaLP MADQLTEEQIAEFKEAFSLFDKDGDGTITTKELGTVMRSLGQNPTEAELHGMISEVDADGNGTIDFPEFLTMMSRK 76
H.sapiens CaM   ADQLTEEQIAEFKEAFSLFDKDGDGTITTKELGTVMRSLGQNPTEAELQDMINEVDADGNGTIDFPEFLTMMARK 75
              **********************************************:.**.******************::*
                                   EF-hand Domain I                    EF-hand Domain II
                 80                  100                 120                 140
H.cumingii CaM  LKDRDSEEELREAFRVFDKDGNGFISAAELRHVMTNLGEKLTDEEVDEMIREADIDGDGQVNYEEFVQMMTSK149
H.cumingii CaLP IKETDTEEEIREAFRVFDKDGNGYISSAELRHVMTNLGEKLTDDEVEEMIKEADVDGDGQVNYEEFVRMMMSK149
H.sapiens CaM   MKDTDSEEEIREAFRVFDKDGNGYISAAELRHVMTNLGEKLTDEEVDEMIREADIDGDGQVNYEEFVQMMTAK148
              :*:  *:***:*************:**:*****************:**:***:***:***********:** :*
                                EF-hand Domain III                  EF-hand Domain IV
```

Fig. 2. Multiple sequence alignment of deduced HcCaM and HcCaLP in *H. cumingii* with CaM in *H. sapiens* (PDB ID: 1CLL). Tree potential phosphorylation sites, 80 aa, 82 aa, and 100 aa, are shaded. The four EF-hand motifs are underlined. The identical (*) and similar (.) or (:) amino acid residues are indicated.

mantle center and foot might also play an important role in the absorption and accumulation of Ca^{2+} (Bevelander, 1952; Tang and Shi, 2000). *hs*CaM from freshwater mussel *H. schlegelii* shared a similar tissue-specific expression pattern (Zeng et al., 2012). Mantle edge is the most active zone for shell formation (Lowenstam and Weiner, 1989). Not only the periostracum is originated from its periostracal groove, but also the prismatic layer is secreted from its outer pallial lobes (Bubel, 1973). In oyster *P. fucata*, CaLP participates in shell formation by inducing the nucleation of aragonite and by regulating growth of calcite in the prismatic layer (Yan et al., 2007; Fang et al., 2008). In the present study, *Hc*CaLP mRNA was mainly expressed in the mantle, especially in the mantle edge, implying that *Hc*CaLP might participate in shell formation of *H. cumingii*.

CaM plays a pivotal role in cellular Ca^{2+} homeostasis by activating Ca^{2+}-ATPase, which is the major transporter in Ca^{2+} fluxes (Snedden and Fromm, 2001; Tine and Kuhl, 2011). The expression of *CaM*s in animals could be induced by environmental stressors, such as hypo-osmotic stress and pathogenic organism (Ji et al., 2011; Tine and Kuhl, 2011). However, the expression of *CaM* in the Pacific oyster *Crassostrea gigas* was down-regulated by low-salinity stress (Zhao et al., 2012). In the present study, the highest transcripts of *Hc*CaM

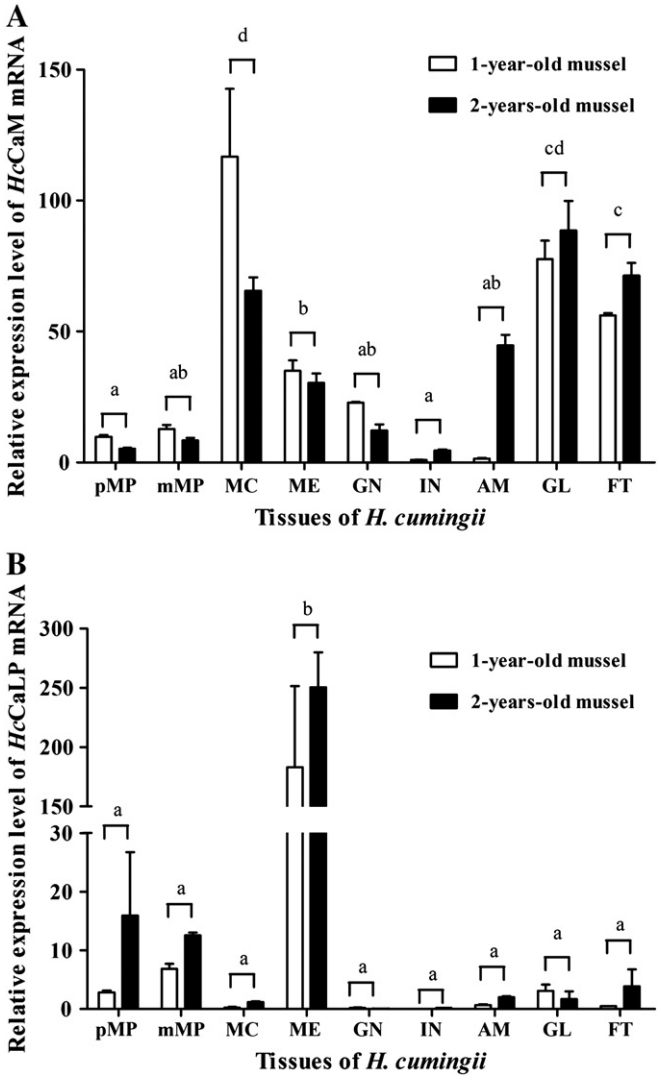

Fig. 3. Expression of *Hc*CaM and *Hc*CaLP mRNA analyzed by real-time PCR in different tissues of 1- and 2-year-old *H. cumingii*. pMP: posterior mantle pallial, mMP: middle mantle pallial, MC: mantle center, ME: mantle edge, GN: gonad, IN: intestine, AM: adductor muscle, GL: gill, FT: foot. *β-actin* was used as an internal control to normalize the expression data. The mRNA levels of 1-and 2-year-old mussels in different tissues are shown as the white columns and black columns, respectively. Data are presented as mean ± SEM (n = 3), and analyzed by a two- way ANOVA with Tukey's HSD test. The difference of mRNA levels in tissues of both 1-and 2-year-old mussels was labeled with different letters ($P < 0.05$). (a) Expression levels of *Hc*CaM mRNA. (b) Expression levels of *Hc*CaLP mRNA.

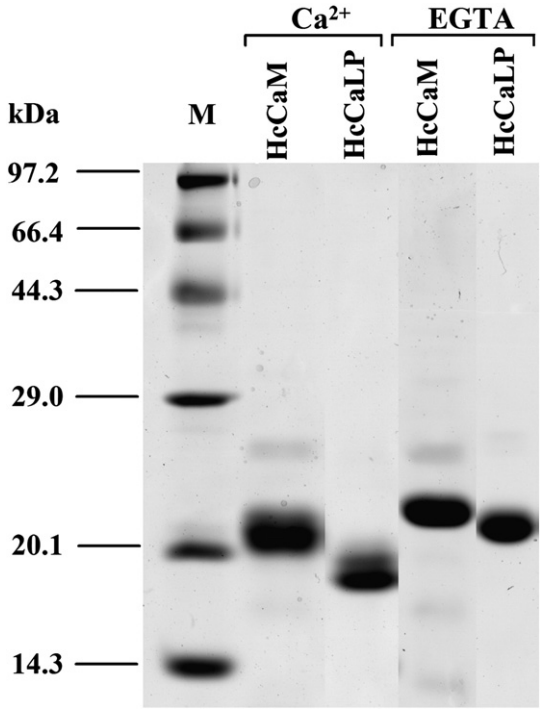

Fig. 4. Ca^{2+}-dependent electrophoretic shift analysis of the purified recombinant proteins HcCaM and HcCaLP. The recombinant proteins were expressed in *E. coli* BL21 (DE3) using a pEASY-E1 expression vector, and induced by 1.0 mM IPTG for 4 h at 37 °C. Recombinant HcCaM and HcCaLP were purified by HisTrap HP affinity column (Ni^{2+} chelating sepharose column). 5 μg purified recombinant proteins were electrophoresed simultaneously in two SDS gels which contained 5 mM CaCl2 or 5 mM EGTA respectively, and stained by Coomassie Brilliant Blue R-250. Protein molecular weight marker is shown on lane M.

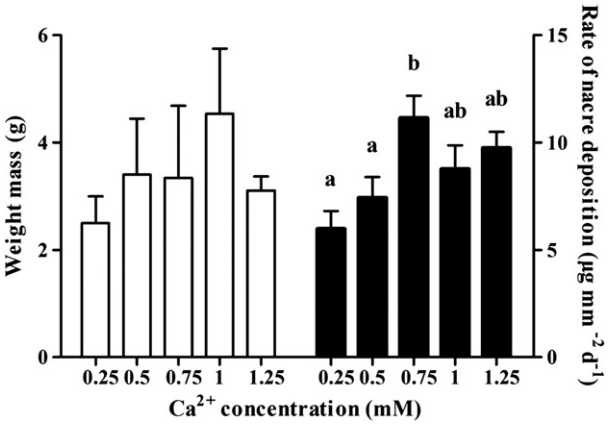

Fig. 5. Mass gain and nacre deposition of 1-year-old *H. cumingii* under different Ca^{2+} concentrations. Mussels were co-cultured with grass carp and crucian carp in 500-liter tanks for 5 weeks. Data are presented as mean ± SEM (n = 10), and the data with different letters are significantly different (Tukey's HSD test, $P < 0.05$).

mRNA under the Ca^{2+} concentration of 0.25 mM suggested that stimulating the *Hc*CaM transcription might help *H. cumingii* to maintain cytosolic Ca^{2+} homeostasis and gain compensatory Ca^{2+} absorption under low Ca^{2+} concentration stress (Fig. 6a). The regulation of CaM to plasma membrane Ca^{2+}-ATPase might play an important role in these processes (Tine and Kuhl, 2011). Moreover, an interesting result in present study is that the relative higher level of *Hc*CaM transcripts at Ca^{2+} concentration of 0.75 mM is consistent with the trend of nacre deposition in shell (see Fig. 5). The expression pattern

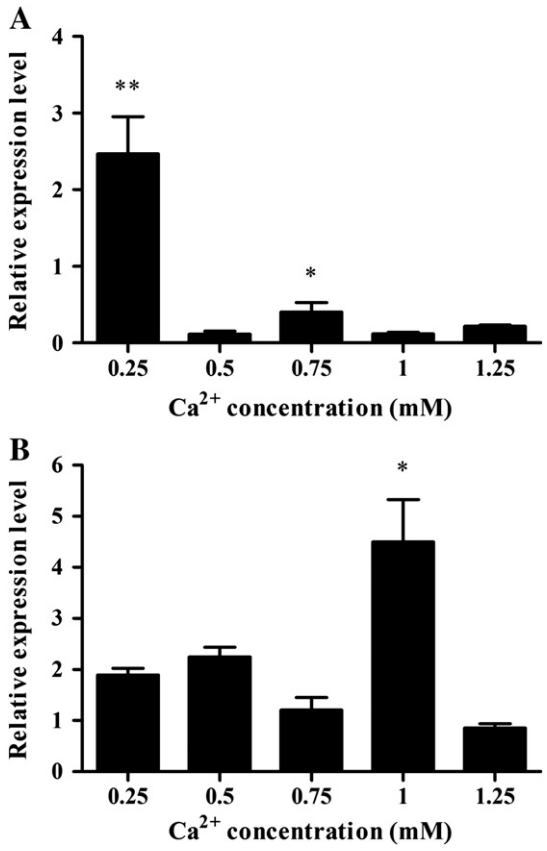

Fig. 6. *Hc*CaM and *Hc*CaLP mRNA expression of 1-year-old *H. cumingii* under different Ca^{2+} concentrations. (a) *Hc*CaLP mRNA expression in gill; (b) HcCaLP mRNA expression in mantle edge. *β-actin* was used as an internal control to normalize the expression data. Mussels were co-cultured with grass carp and crucian carp in 500-liter tanks for 5 weeks. Data are expressed as mean ± SEM (n = 3), and the data with different letters are significantly different (Tukey's HSD test, $P < 0.05$).

of *Hc*CaM mRNA in *H. cumingii* under different Ca^{2+} concentrations reveals the complexity of regulation of *Hc*CaM expression, which might be closely related with the functions of HcCaM as a versatile calcium signal transducer. In contrast to high *Hc*CaM mRNA transcripts in gill at Ca^{2+} concentration of 0.75 mM, the highest expression level of *Hc*CaLP in mantle edge occurred at 1 mM (see Fig. 6b), suggesting the differential expression of *Hc*CaM and *Hc*CaLP mRNA in response to Ca^{2+} concentration. Therefore, the expression of *Hc*CaM mRNA and *Hc*CaLP mRNA in *H. cumingii* is affected by Ca^{2+} concentrations, and the Ca^{2+} concentrations of 0.75 to 1 mM are suitable for shell growth of the mussel.

In conclusion, the full-length cDNAs of *Hc*CaM and *Hc*CaLP in *H. cumingii* were described. The important mutation sites between HcCaM and HcCaLP are located in the potential phosphorylation sites aa^{80} and aa^{100}. HcCaM and HcCaLP differ in the calcium binding affinity. *Hc*CaM and *Hc*CaLP mRNA can expressed in different tissues, including gill, intestine, foot, gonad adductor muscle and mantle pallial, and *Hc*CaM and *Hc*CaLP mRNA expression is affected by environmental Ca^{2+} concentrations.

Acknowledgments

We thank Prof. Jinrong Peng and Dr. Yi-hong Guan for assistance in RT-PCR technology. This work was funded by the National Basic Research Program of China (2009CB118705).

References

Bevelander, G., 1952. Calcification in molluscs. 3. Intake and deposition of Ca^{45} and P^{32} in relation to shell formation. Biol. Bull. US 102, 9–15.
Breimer, L.H., MacIntyre, I., Zaidi, M., 1988. Peptides from the calcitonin genes: molecular genetics, structure and function. Biochem. J. 255, 377–390.
Bubel, A., 1973. An electron-microscope study of periostracum formation in some marine bivalves. I. The origin of the periostracum. Mar. Biol. 20, 213–221.
Burgess, W.H., Jemiolo, D.K., Kretsinger, R.H., 1980. Interaction of calcium and calmodulin in the presence of sodium dodecyl sulfate. Biochim. Biophys. Acta 623, 257–270.
Corti, C., Leclerc, L.E., Quadroni, M., Schmid, H., Durussel, I., Cox, J., Dainese, H.P., James, P., Carafoli, E., 1999. Tyrosine phosphorylation modulates the interaction of calmodulin with its target proteins. Eur. J. Biochem. 262, 790–802.
Dalesman, S., Lukowiak, K., 2010. Effect of acute exposure to low environmental calcium on respiration and locomotion in *Lymnaea stagnalis* (L.). J. Exp. Biol. 213, 1471–1476.
Duplat, D., Puissegur, M., Bedouet, L., Rousseau, M., Boulzaguet, H., Milet, C., Sellos, D., Van Wormhoudt, A., Lopez, E., 2006. Identification of calconectin, a calcium-binding protein specifically expressed by the mantle of *Pinctada margaritifera*. FEBS Lett. 580, 2435–2441.
Fang, Z., Cao, W., Li, S., Wang, Q., Li, C., Xie, L., Zhang, R., 2008. Significance of the C-terminal globular domain and the extra tail of the calmodulin-like protein (*Pinctada fucata*) in subcellular localization and protein-protein interaction. Cell Biol. Int. 32, 920–927.
Friedberg, F., Rhoads, A.R., 2001. Evolutionary aspects of calmodulin. IUBMB Life 51, 215–221.
Hoeflich, K.P., Ikura, M., 2002. Calmodulin in action: diversity in target recognition and activation mechanisms. Cell 108, 739–742.
Huang, J., Zhang, C., Ma, Z., Xie, L., Zhang, R., 2007. A novel extracellular EF-hand protein involved in the shell formation of pearl oyster. Biochim. Biophys. Acta 1770, 1037–1044.
Ikura, M., Ames, J., 2006. Genetic polymorphism and protein conformational plasticity in the calmodulin superfamily: two ways to promote multifunctionality. Proc. Natl. Acad. Sci. U. S. A. 103, 1159–1164.
Ji, P.F., Yao, C.L., Wang, Z.Y., 2011. Two types of calmodulin play different roles in Pacific white shrimp (*Litopenaeus vannamei*) defenses against Vibrio parahaemolyticus and WSSV infection. Fish Shellfish Immunol. 31, 260–268.
Kilhoffer, M.C., Haiech, J., Demaille, J.G., 1983. Ion binding to calmodulin. A comparison with other intracellular calcium-binding proteins. Mol. Cell. Biochem. 51, 33–54.
Lee, S.H., Johnson, J.D., Walsh, M.P., Van Lierop, J.E., Sutherland, C., Xu, A., Snedden, W.A., Kosk-Kosicka, D., Fromm, H., Narayanan, N., Cho, M.J., 2000. Differential regulation of Ca^{2+}/calmodulin-dependent enzymes by plant calmodulin isoforms and free Ca^{2+} concentration. Biochem. J. 350, 299–306.
Li, S., Xie, L., Zhang, C., Zhang, Y., Gu, M., Zhang, R., 2004. Cloning and expression of a pivotal calcium metabolism regulator: calmodulin involved in shell formation from pearl oyster (*Pinctada fucata*). Comp. Biochem. Physiol. B 138, 235–243.
Li, S., Xie, L., Ma, Z., Zhang, R., 2005. cDNA cloning and characterization of a novel calmodulin-like protein from pearl oyster *Pinctada fucata*. FEBS J. 272, 4899–4910.
Lowenstam, H., Weiner, S., 1989. On Biomineralization. Oxford University Press, New York.
Machado, J., Lopes-Lima, M., 2011. Calcification mechanism in freshwater mussels: potential targets for cadmium. Toxicol. Environ. Chem. 93, 1778–1787.

Nikapitiya, C., De Zoysa, M., Whang, I., Kim, S.J., Choi, C.Y., Lee, J.S., Lee, J., 2010. Characterization and expression analysis of EF hand domain-containing calcium-regulatory gene from disk abalone: calcium homeostasis and its role in immunity. Fish Shellfish Immunol. 29, 334–342.

Ojima, T., Tanaka, H., Nishita, K., 1994. Cloning and sequence of a cDNA encoding Akazara scallop troponin C. Arch. Biochem. Biophys. 311, 272–276.

Richardson, C.A., Runham, N.W., Crisp, D.J., 1981. A histological and ultrastructural study of the cells of the mantle edge of a marine bivalve, *Cerastoderma edule*. Tissue Cell 13, 715–730.

Rogers, M.S., Kobayashi, T., Pittelkow, M.R., Strehler, E.E., 2001. Human calmodulin-like protein is an epithelial-specific protein regulated during keratinocyte differentiation. Exp. Cell Res. 267, 216–224.

Sidhu, K.S., Guraya, S.S., 1993. Effect of calmodulin-like protein from buffalo (*Bubalus bubalis*) seminal plasma on Ca^{2+}, Mg^{2+}-ATPase of purified plasma membrane of buffalo spermatozoa. Andrologia 25, 25–28.

Simpson, R.J., Wilding, C.S., Grahame, J., 2005. Intron analyses reveal multiple calmodulin copies in *Littorina*. J. Mol. Evol. 60, 505–512.

Snedden, W.A., Fromm, H., 2001. Calmodulin as a versatile calcium signal transducer in plants. New Phytol. 151, 35–66.

Stommel, E.W., Stephens, R.E., 1985. Calcium-dependent phosphatidylinositol phosphorylation in lamellibranch gill lateral cilia. J. Comp. Physiol. A 157, 441–449.

Stommel, E.W., Stephens, R.E., Masure, H.R., Head, J.F., 1982. Specific localization of scallop gill epithelial calmodulin in cilia. J. Cell Biol. 92, 622–628.

Tang, M., Shi, A., 2000. Studies of environmental calcium concentration effect on the calcium metabolism of the mantle and pearel sac of the freshwater pearl mussel. J. Sichuan Univ. 37, 741–747.

Thompson, J.D., Higgins, D.G., Gibson, T.J., 1994. CLUSTAL W: improving the sensitivity of progressive multiple sequence alignment through sequence weighting, position-specific gap penalties and weight matrix choice. Nucleic Acids Res. 22, 4673–4680.

Tine, M., Kuhl, H., 2011. Changes in calmodulin gene expression in the gills of the black-chinned tilapia *Sarotherodon melanotheron* from drainage basins with different salinities. Int. Res. J. Biotechnol. 2, 9–15.

Toutenhoofd, S.L., Strehler, E.E., 2000. The calmodulin multigene family as a unique case of genetic redundancy: multiple levels of regulation to provide spatial and temporal control of calmodulin pools? Cell Calcium 28, 83–96.

Wang, Y., Wang, W.L., Qin, J.G., Wang, X.D., Zhu, S.B., 2009. Effects of integrated combination and quicklime supplementation on growth and pearl yield of freshwater pearl mussel, *Hyriopsis cumingii* (Lea, 1852). Aquac. Res. 40, 1634–1641.

Wei, F.S., 2002. Monitoring and Analysis Method of Water and Wastewater. China Envir. Sci. Press, Beijiang.

Wilbur, K.M., Jodrey, L.H., 1952. Studies on shell formation. I. Measurement of the rate of shell formation using Ca^{45}. Biol. Bull. 103, 269–276.

Yan, Z., Fang, Z., Ma, Z., Deng, J., Li, S., Xie, L., Zhang, R., 2007. Biomineralization: functions of calmodulin-like protein in the shell formation of pearl oyster. Biochim. Biophys. Acta 1770, 1338–1344.

Zeng, L.G., Wang, J.H., Li, Y.J., Sheng, J.Q., Gu, Q., Hong, Y.J., 2012. Molecular characteristics and expression of calmodulin cDNA from the freshwater pearl mussel, *Hyriopsis schlegelii*. Genet. Mol. Res. 11, 42–52.

Zhao, X., Yu, H., Kong, L., Li, Q., 2012. Transcriptomic responses to salinity stress in the Pacific oyster *Crassostrea gigas*. PLoS One 7, e46244.